Journal of Thermal Analysis and Calorimetry, Vol. 57 (1999) 631-642

POLYMORPHISM OF ACRYLIC AND METHACRYLIC ACID ESTERS CONTAINING LONG FLUOROCARBON CHAINS AND THEIR POLYMERIZABILITY

A. Fujimori, H. Saitoh and Y. Shibasaki

Department of Chemistry, Faculty of Science, Saitama University, 255 Shimo-okubo Urawa, 338-8570, Japan

Abstract

The molecular aggregation of acrylic and methacrylic acid esters containing long-fluorocarbon chains: 2-(perfluoroalkyl)ethyl acrylate (FF_nEA) and 2-(perfluoroalkyl)ethyl methacrylate (FF_nEMA) ($F(CF_2)_nCH_2CH_2OCOC(X)=CH_2$, where *X*=H, CH_3 and *n*=6, 8, 10) was investigated by differential scanning calorimetry (DSC) and temperature controlled X-ray powder diffraction measurement. These compounds exhibited some characteristic polymorphic behaviors depending on the length of fluorocarbon chain and the α-position methyl group. The solid-state polymerization by γ-ray irradiation was studied for these compounds in the various crystal forms. In the solid-state polymerization, highest polymerizability was observed in the crystal form that exists in the highest temperature region for each compound.

Keywords: DSC, fluorocarbon chain, polymerizability, polymorphic behaviors, X-ray diffraction

Introduction

The comb polymers containing fluorocarbon chain in the side chains have been used on several fields as oil-resistant rubbers for using at high temperature, and fluorine manufactured products. The character of these polymers containing fluorocarbon chains has been based on the properties of fluorocarbon chain such as good rubbing-resistant, chemical-resistant and surface activity. Fluorocarbon chain is thicker and less flexible than hydrocarbon chain, since the van der Waals radius of fluorine atom is too large to allow of making precise trans zig-zag planar conformation of $–(CF_2–CF_2)_n–$ chain, as the poly(tetrafluoroethylene) [1–7]. Budovskaya *et al*. synthesized some monomer molecules containing long fluorocarbon chains which have tendency to make some layer structures [8]. We had investigated the molecular aggregation state and the γ-ray irradiation solid state polymerization for the acrylate and methacrylate compounds containing fluorocarbon chains ($H(CF_2)_nCH_2OCO(X)=CH_2$; F_nA and F_nMA, where *X*=H, CH_3 and *n*=4, 6, 8, 10) [9–10], and else studied the polymorphism of long-chain monomer compounds containing hydrocarbon chain [11–12]. We found very few reports on the change of the powder diffraction patterns depending on the polymorphic behavior for long-chain compounds, because these compounds are mostly wax like state and hard to make even powder sample to say

1418–2874/99/ $ 5.00

Akadémiai Kiadó, Budapest
Kluwer Academic Publishers, Dordrecht

nothing of very thin single crystal. In this study, molecular aggregations and polymorphic behaviors of 2-(perfluoroalkyl)ethyl acrylate (FF_nEA) and 2-(perfluoroalkyl)ethyl methacrylate (FF_nEMA) ($F(CF_2)_nCH_2CH_2OCOC(X)=CH_2$, where *X*=H, CH_3 and *n*=6, 8, 10), which is analogues of F_nA and F_nMA concerning the terminal H atom in fluorocarbon chain was fluorinated and the methylene group was substituted the ethylene group, are investigated by DSC and X-ray powder diffraction measurement, and the influence of polymorphism of these compounds on their γ-ray irradiation polymerization are also studied and discussed.

Experimental

Materials

The materials were purchased from Daikin Fine Chemicals. Samples were purified by recrystallizations repeated sixth ~ ninth times from *n*-hexane solution for all measurements. Although FF_6EA, FF_6EMA, FF_8EA and FF_8EMA are liquid state at room temperature, the recrystallizations were carried out from cold *n*-hexane solution cooled by immersing into liquid-solid coexistence system of chloroform at –63.5°C and that of ethyl acetate at –83.6°C for FF_6EA and FF_6EMA.

Methods for studying polymorphism

The thermal analyses were carried out using a Seiko Instruments model DSC6200 differential scanning calorimeter with a liquid N_2 cooling system. The DSC measurements were performed with a scanning rate of 2.0°C min^{-1} as standard. Sample mass of ca 1.50 mg was used for all DSC measurements. The temperature range of the scanning was selected to include sufficiently the important information of all phase transitions for each compound, and the scanning was performed once down to low temperature limit (about –150°C) determined by the ability of the cooling apparatus. As usual scanning of DSC measurements, heating and cooling cycle was repeated three times, in order to examine for the difference of the peak position and the transition enthalpy between first heating and after that. This phenomenon is caused by the difference of thermal stability of the crystalline phase between that recrystallized from the solution and that recrystallized from the melt by cooling. In addition, we performed that the heating or cooling process reversed quickly after a transition peak appeared for every peak, because the character of the phase transitions should be clarified. Transition enthalpy was calculated from the peak area on DSC curve, and the transition entropy was calculated from dividing the enthalpy value by absolute temperature of the phase transition.

The packing modes of the molecules in crystalline phase were examined by X-ray powder diffraction measurement using a Mac Science MXP18VA diffractometer with CuK_α radiation, which equipped with a graphite monochrometer, 40 kV, 100 mA. This apparatus also equipped with heating and cooling attachment that using liquid N_2. X-ray diffraction measurements of present work were performed on the same temperature range of DSC measurements for the corresponding compound.

Polymerization procedure

Solid-state postpolymerization were carried out at various temperatures (–83.6 ~ 50°C). The monomer samples of about 0.5 mg were sealed in Pyrex glass tubes (inside diameter 10 mm) in a vacuum or nitrogen atmosphere, and irradiated with ^{60}Co γ-rays (1.0 Mrad in liquid N_2) at –196°C (Scheme 1). These samples were polymerized for fixed periods (0.5, 1, 2, 3, 6 and 12 h) and dissolved in 2 ml of acetone and poured into 50 ml of CCl_4 to deposit poly(FF_nEA) and poly(FF_nEMA) [13–14]. The precipitate of the polymer was isolated by glass filter and its conversion was determined from the mass of the polymer obtained after drying under vacuum at room temperature. The γ-ray irradiation was carried out at the Japan Atomic Energy Institute at Takasaki.

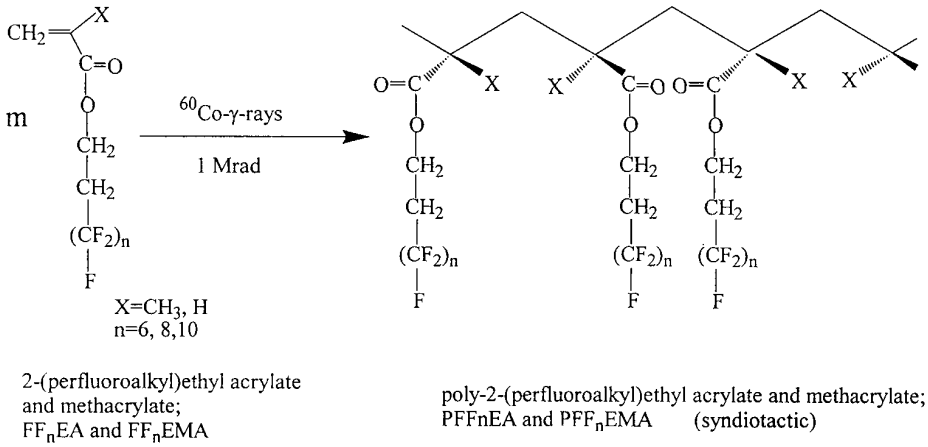

Scheme 1 Solid-state polymerization of FF_nEA and FF_nEMA

Results and discussion

Polymorphic behaviors of FF_nEA and FF_nEMA

a) The case of FF_8EA and FF_8EMA

First, the case of FF_8EA and FF_8EMA, which exhibit clearly polymorphism, are discussed. The DSC curves for FF_8EA and FF_8EMA are shown in Fig. 1. FF_8EA showed two transition peaks on both heating and cooling processes. The transition enthalpy of both melting and crystallization peaks at about –5°C was ΔH= 6.6 kJ mol^{-1} and that of other transition peaks between different crystal forms at –20°C on heating and at –40°C on cooling was the same ΔH=6.9 kJ mol^{-1}. On the other hand, FF_8EMA showed two transition-peaks on cooling process, too, but it showed only one transition peak on heating process. The transition enthalpies of crystallization at –15°C and additional transition at –40°C on cooling process were

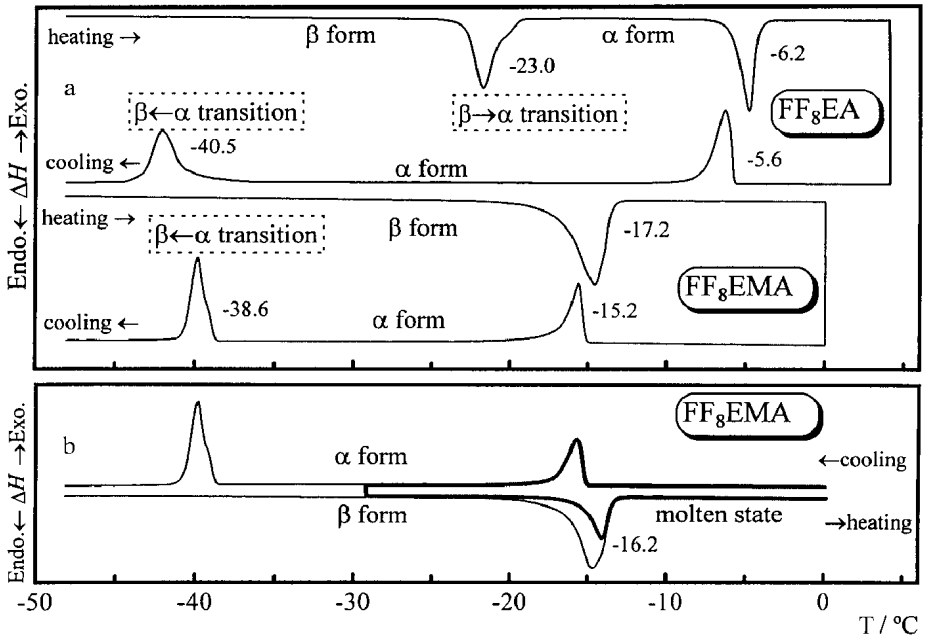

Fig. 1 a) DSC curves for FF_8EA and FF_8EMA; b) The influence of the scanning process quickly changed on DSC curves for FF_8EMA

ΔH=6.1 and 9.5 kJ mol^{-1}, respectively. The enthalpy of fusion was ΔH=15.6 kJ mol^{-1} and the value was nearly equal to the sum of those for two transition peaks on cooling process. According to the Larsson's rule [15], first crystal form obtained from liquid state on cooling is named 'α form', and a most stable state, which appeared via next transition below about –45°C, is named 'β form' for both FF_8EA and FF_8EMA. Figure 1(b) shows the influence of the scanning process reversed quickly between the crystallization and the transition peaks for FF_8EMA. The melting point on this scanning was increased as compared with that on usual scanning, and the enthalpy was decreased to ΔH=6.1 kJ mol^{-1}, which was the same value for the crystallization. We think that the melting peak for FF_8EMA on usual scanning was the melting of β form and the peak on reversed scanning was the melting of α form. The polymorphism of FF_8EMA was a monotropic phase transition. On the other hand, since the similar technique on DSC measurements for FF_8EA was performed, it was found that the transition behavior was enantiotropic. In the case of FF_8EMA, 'α form' was not appeared on heating process, while in FF_8EA 'α form' was appeared on both heating and cooling processes. Although the difference of the molecular structure is little, some effects of bulky α-position methyl group cause the difference between the transition behaviors of two compounds.

Figure 2 shows X-ray powder diffraction patterns for FF_8EA and FF_8EMA in each crystal form. It shows clearly that the structural change was brought by the

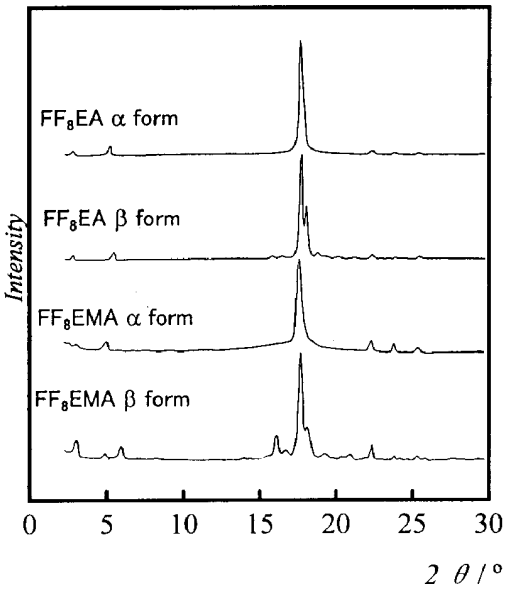

Fig. 2 Powder patterns for FF_8EA and FF_8EMA in temperature controlled X-ray diffraction

solid-to-solid phase transitions. The powder patterns for FF_8EA and FF_8EMA exhibited that main structural change of these compounds was the change of packing mode between hexagonal and orthorhombic in two-dimensional lattice.

Figure 3 shows schematic diagrams of the Gibbs energy-temperature relationship and the entropy-temperature one for FF_8EA (a) and FF_8EMA (b). These diagrams indicate the energy relationships of crystalline modifications for FF_8EA and FF_8EMA. In the view of energy relationship, both compounds exhibited large entropy change on $\alpha \rightarrow \beta$ transition, which was no less large than $\alpha \leftrightarrow$liquid transition. It is supposed that the change of crystal structure for $\alpha \rightarrow \beta$ transition, which was the change from the hexagonal packing mode to the orthorhombic one, occurred with relatively large decreasing of entropy. Besides, the entropy change of fusion might be small due to less degree of freedom on the rigid fluorocarbon chain. The main difference of FF_8EA and FF_8EMA in Fig. 3 was that whether the phase transition behavior occurred via α form on heating process, or not. Figure 3(a) shows the enantiotropic phase transition behavior of FF_8EA, which always transited via α form on both heating and cooling processes. In addition, large hysteresis was observed for the $\alpha \leftrightarrow \beta$ transition probably because the nucleation of β form crystal took a relatively long time. On the other hand, Fig. 3(b) shows the monotropic phase transition behavior of FF_8EMA, which directly melted from β form to liquid state on heating process without $\beta \rightarrow \alpha$ transition. However, after the crystallization into α form on cooling process, the change of scanning to heating process could cause enantiotropic $\alpha \leftrightarrow$ liquid transition (ΔS=25.7 J $K^{-1}mol^{-1}$).

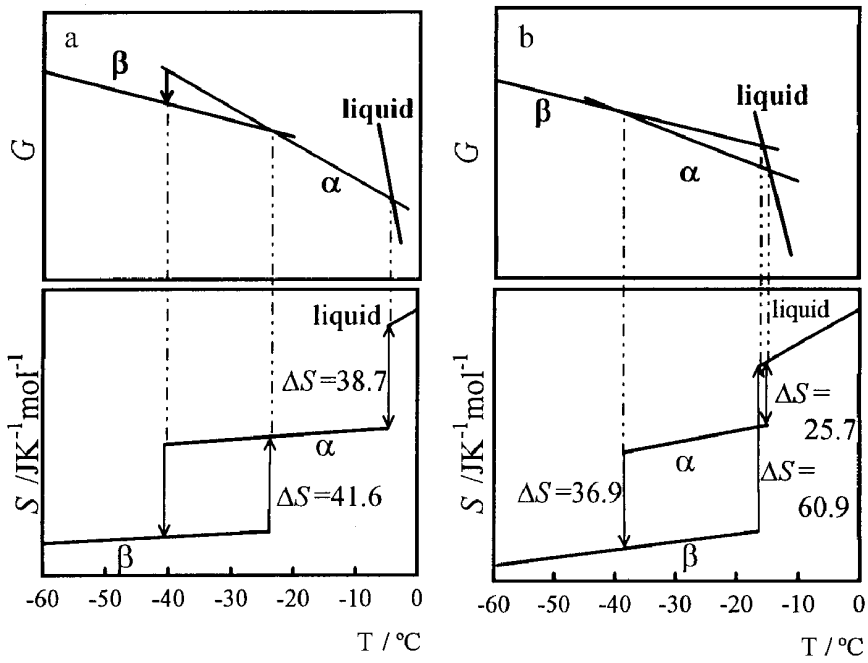

Fig. 3 Schematic diagrams for the Gibbs energy-temperature and entropy-temperature relationships of FF_8EA (a) and FF_8EMA (b)

According to these results, the phase transition behaviors and the cross-section diagrams viewed along the molecular axis for FF_8EA and FF_8EMA illustrated schematically in Fig. 4.

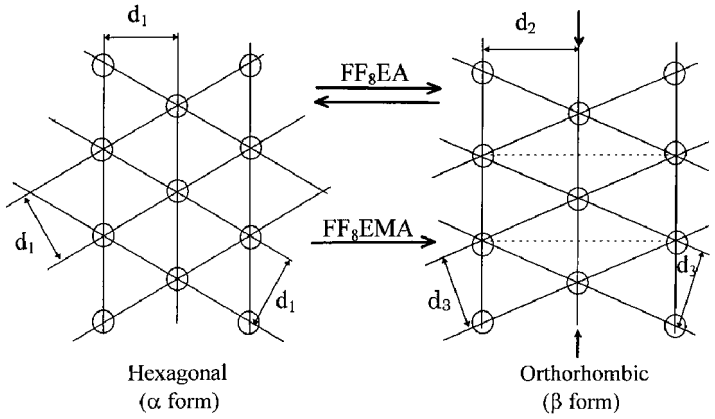

Fig. 4 Phase transition behavior of FF_8EA and FF_8EMA and change of structure for two-dimensional cell; on hexagonal form, $a=b$, lattice angle $\gamma=120°$, $d_1=4.99(FF_8EA)$, $d_1=5.03(FF_8EMA)$; on orthorhombic form, lattice angle $\alpha=\beta=\gamma$, $d_2=4.98$, $d_3=4.89(FF_8EA)$, $d_2=5.00$, $d_3=4.87(FF_8EMA)$

b) The case of the compounds having longer fluorocarbon chain

The DSC curves for $FF_{10}EA$ and $FF_{10}EMA$ having longer fluorocarbon chains are shown in Fig. 5, and those are very similar each other at first glance. On the curves, the melting and crystallization peaks were observed for $FF_{10}EA$ and $FF_{10}EMA$ at about 50 and 40°C, respectively. In addition, some solid-to-solid transition peaks with very small transition enthalpies appeared in the lower temperature region. However, the curves of $FF_{10}EMA$ was different from those of $FF_{10}EA$ in the point of the plural transition peaks founded in the range of 15~30°C on both heating and cooling processes. Figure 6 shows X-ray powder diffraction patterns at several temperatures for $FF_{10}EA$ (a) and $FF_{10}EMA$ (b). The both compounds were commonly observed high-intensity plural long spacing diffraction peaks with higher order reflections, and it means the firmly grown layer structures because of the favorable nature of longer chain for crystallizing.

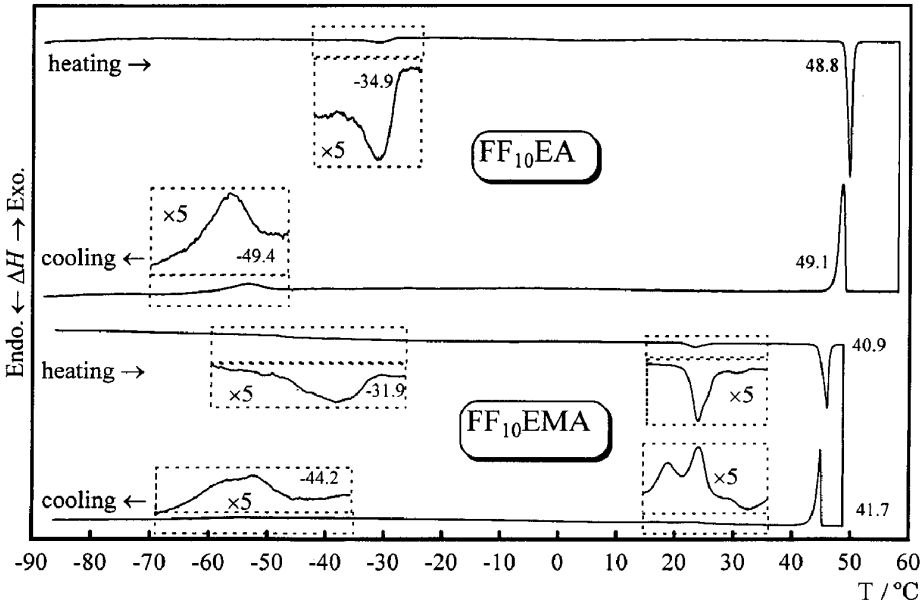

Fig. 5 DSC curves for $FF_{10}EA$ and $FF_{10}EMA$

Firstly, we describe in detail for $FF_{10}EMA$. Figure 6(c) shows the change of the long spacing diffraction peaks in small angle region at various temperatures. In higher temperature region above 20°C, it can be considered that the peak at $2\theta=4°$ corresponds to the molecular length of $FF_{10}EMA$ about 20 Å for first order reflection. However, in lower temperature region below 15°C, new first order reflection appeared at d=ca 40 Å and it accompanied with new odd orders reflections. Thus, the peak at about 20 Å seems to be second order reflection with showing shift of the position toward higher angle. These results suggest that a double-layer structure formed in lower temperature region for $FF_{10}EMA$. It is an improbable phenomenon

that $FF_{10}EMA$ molecule turn over suddenly at this temperature about 20°C because of the very small transition enthalpy (ΔH=1.5 kJ mol^{-1}). Hence, we suppose that in the higher temperature phase the double layer structure is hard to confirm by the X-ray diffraction method due to the influence of large thermal motion of the molecules, thus the diffraction pattern looks like of a single layer structure. In the further lower temperature DSC curves, the peaks at –35°C on heating process and at –55°C on cooling are also related to the change of X-ray diffraction pattern, and the diffraction peaks profile was broaden and weaken below the transition temperature. It can be considered that the expansion of the layer structure collapses for $FF_{10}EMA$ in higher temperature region via the phase transition, though the transition enthalpy (ΔH=1.5 kJ mol^{-1}) was very small.

For $FF_{10}EA$, the X-ray diffraction patterns for long spacing in Fig. 6(a) indicate that this compound has double layer structure among all temperatures, and it is different from the case of $FF_{10}EMA$. The change of the X-ray diffraction pattern, that is, the short spacing peak was split into d=4.93 and 4.86 Å was found for $FF_{10}EA$ at

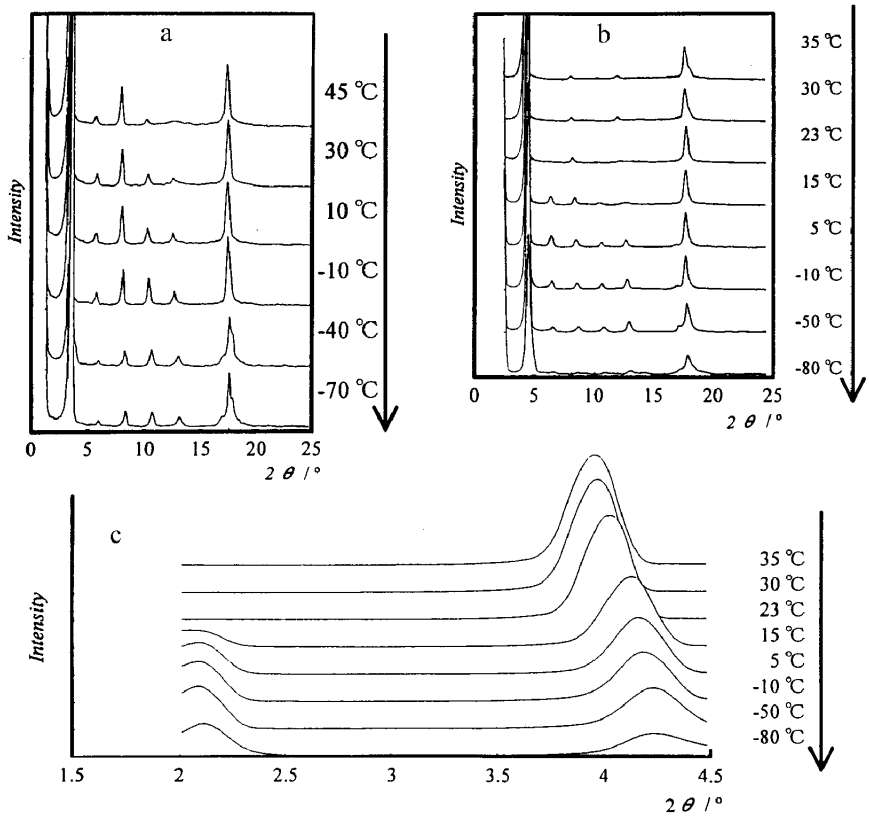

Fig. 6 Powder patterns for $FF_{10}EA$ and $FF_{10}EMA$ in temperature controlled X-ray diffraction: a) $FF_{10}EA$, b) $FF_{10}EMA$, c) Change of the long spacing peaks of $FF_{10}EMA$ in X-ray powder diffraction on several temperatures

low temperature. This change could be related to the solid-solid phase transition at about –50°C on DSC measurement. The peak splitting means the transformation from hexagonal packing for high-temperature phase to orthorhombic one for low-temperature phase. Moreover, the short spacing peaks of this compound in the lower temperature region below –60°C would be broad. In addition, the intensities of high-order long spacing reflections were increased with decreasing temperature, which means the growth of layer structure. All long spacing reflections have tendency to shift to larger angle with cooling, which means that the long molecular axis has been tilted. This tendency was same for $FF_{10}EMA$. Additional new long spacing peaks, which meant existence of the more tilted molecule, appeared, too.

c) The case of the compounds having shorter fluorocarbon chain

The DSC curves for FF_6EA and FF_6EMA having shorter fluorocarbon chains are shown in Fig. 7(a). In the case of FF_6EA, both exo- and endothermic peaks appeared on heating process, and an exothermic peak appeared on cooling process at about –60°C. Small exothermic peak on heating process was located at about the same temperature for the crystallization peak on cooling process. Hence, we guessed that this phenomenon occurred because the crystal nucleation did not proceed sufficiently in the time scale of the cooling process. In other words, the exothermic peak on heating process was meant that the crystal transited to more stable phase on heating process, and the transition could not be enough to stabilize on cooling process. It had been observed similar phenomenon for F_6A. For F_6A, exo- and endothermic peaks appeared on only heating process, however, no crystallization peak was ob-

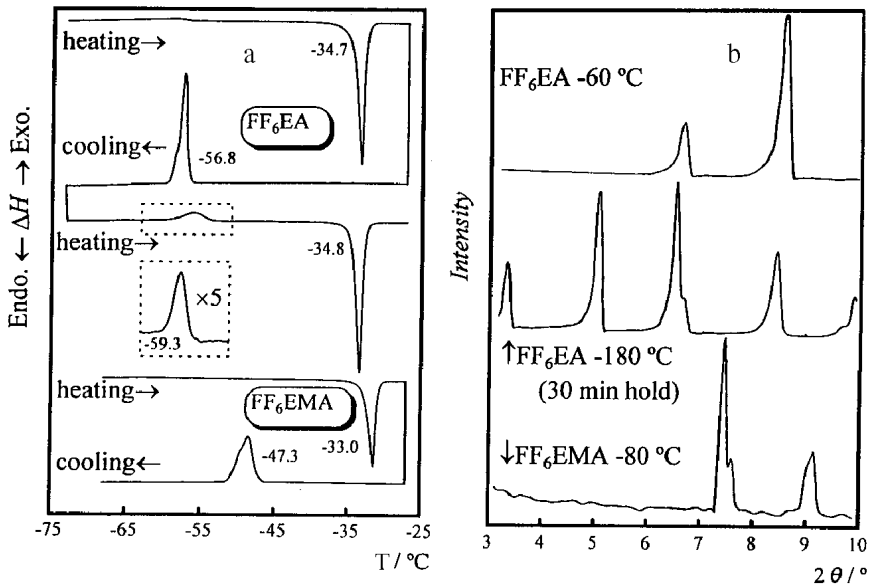

Fig. 7 a) DSC curves for FF_6EA and FF_6EMA. b) Powder patterns for long spacing peaks of FF_6EA and FF_6EMA in temperature controlled X-ray diffraction

served on cooling process [9–10]. In the case of F_6A, the crystal nucleation had never occurred in the time scale of the measurements because of shorter length of F_6A molecule than FF_6EA.

On the other hand, it seemed that the rate of crystal growth for FF_6EMA was enough to stabilize the crystal in the time scale of cooling process though this compound did not show polymorphic behavior. FF_6EMA exhibited only one transition peak on the each heating and cooling process. This result means that the chemical structure of FF_6EMA was convenient to form the stabilized crystal with higher melting point than that of FF_6EA (Fig. 7(a)) because of existence of bulky α-position methyl group.

Figure 7(b) shows X-ray powder diffraction patterns for FF_6EA and FF_6EMA. For FF_6EA, long spacing peaks not appeared more than 13.4 Å: one molecular length of this compound, on –60°C. However, after about 30 min holding at temperature of –180°C, two long spacing peaks appeared in the position of 27.8 and 17.9 Å. Hence, it was found that this compound could form the stable double layer structure by storing for long time at a low temperature, though the rate of crystal growth for this compound was too slow to form double layer structure in the time scale of DSC measurements. No long spacing peaks appeared for FF_6EMA more than 11.8 Å, which was shorter than the molecular length of even FF_6EA. Hence, we could consider that the existence of bulky α-position methyl group increased crystallinity, although prevented formation of layered structure, that is the same case of $FF_{10}EMA$. This assumption was proved by the relationships between polymerizabilities and crystal forms for FF_6EA and FF_6EMA (Fig. 8).

As mentioned above, it was found that all compounds studied in this work exhibited characteristic phase transition behaviors which didn't observed for F_nA and F_nMA because of the effect of increasing molecular flexibility caused by the difference of ethylene group from methylene group.

Effect of the polymorphism on solid state polymerization

Figure 8 shows the saturated conversion-polymerization temperature curves for FF_nEA and FF_nEMA. The conversions of $FF_{10}EA$ and $FF_{10}EMA$ limited to 20~30% because of the effect of molecular packing in lamellar structure which restrains kinetic freedom of C=C bond. On the other hand, in the case of FF_6EA and FF_8EA active motion of functional groups for polymerization achieved high conversion. While, the conversion of FF_8EMA extremely increased up to 70% above the melting point, though the conversion was about 40% in lower temperature. This is explained by a conventional mechanism for the irradiation polymerization in solid-state. Hence, the thermal motion of C=C bond have become active, because the freedom of C=C bond, which restrained by α-position methyl group in lower temperature, increases with polymerization temperature [5].

The conversion of FF_6EMA abruptly decreased above the melting point, and it differed from another compounds. Generally, highest conversion of the long chain compounds was observed at a little higher temperature than melting point. This is

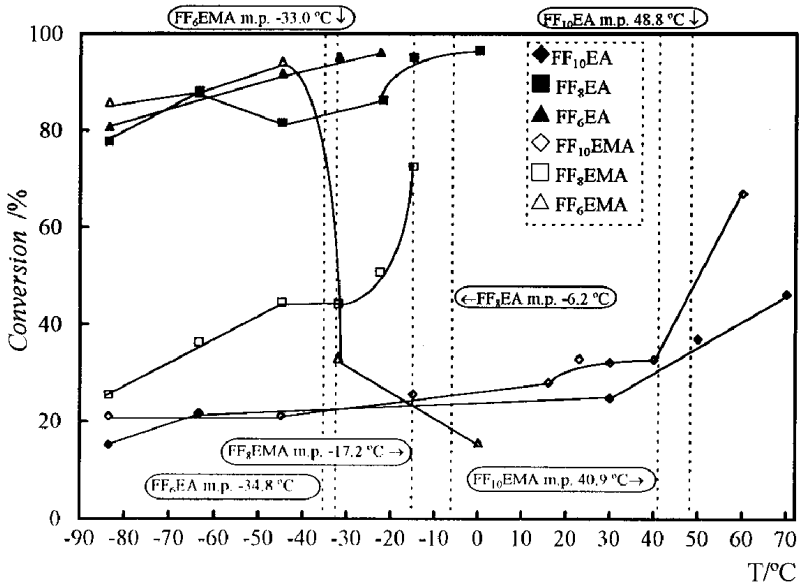

Fig. 8 Saturated conversion-polymerization temperature curves for FF_nEA and FF_nEMA

because layered structure of the long chain compounds retains until a little higher temperature than melting point [16–18]. In comparison with FF_6EA, FF_6EMA had excellent crystallinity by α-position methyl group (Fig. 7). However, according to our assumption, that is, the bulky methyl group at α-position prevented the development of layered structure, the disordering of layered structure relatively promoted by existence of bulky α-position methyl group, caused the decrease of conversion above the melting point of FF_6EMA. This assumption was agreed well with the result of the X-ray powder diffraction for FF_6EMA, which could not form double layer structure (Fig. 7(b)).

In the solid-state polymerization of these compounds except FF_6EMA, highest polymerizability was observed in the crystal form in highest temperature region or just above the melting point of every compound because of increasing rotational freedom of functional group. This result almost corresponds with the previous report of long hydrocarbon chain vinyl esters [16–18].

References

1 N. A. Platé and V. P. Shibaev, J. Polym. Sci., Macromol. Rev., 8 (1974) 117.
2 N. A. Platé and V. P. Shibaev, 'Comb-Shaped Polymers and Liquid Crystals', Plenum, New York 1987.
3 J. Schneider, C. Erdelen, H. Ringsdorf and H. Rabolt, Macromolecules, 22 (1989) 3475.
4 Y. Shibasaki and K. Fukuda, Thermochim. Acta, 88 (1985) 211.
5 Y. Shibasaki, Thermochim. Acta, 123 (1988) 191.
6 Y. Shibasaki, R. Horie, T. Takahashi and Y. Ichimura, Thermochim. Acta, 282/283 (1996) 425.

7 Y. Shibasaki, 'Comb-like Polymers', Polymeric Materials Encyclopedia, Ed., J. C. Salamone, Vol. 2, CRC Press., New York 1996, pp. 1336–1342.
8 L. D. Budovskaya, V. N. Ivanova and L. N. Oskar, Polym. Sci. U.S.S.R, 32 (1990) 502.
9 Y. Shibasaki, H. Saitoh and K. Chiba, J. Thermal Anal., 49 115 (1997).
10 Y. Shibasaki and H. Saitoh, Polymer Preprints, Japan, 47 (1998) 255.
11 Y. Shibasaki, Proc. 7th ICTA, 1982, Vol. 2, Thermal Analysis, Bernard, Miller, Wiley, 1982, p. 1517.
12 Y. Shibasaki, Netsu Sokutei, 12 (1985) 116.
13 Y. Shibasaki and Z. Q. Zhu, JAERI-Conf. 95, Proc. 6th Japan-China Bilateral Symposium on Radiation Chemistry, Tokyo 1994, p. 275.
14 Y. Shibasaki, Z. Q. Zhu and K. Fukuda, J. Nanjing Univ. (Natural Sci. Ed.), 31 (1995) 335.
15 K. Larsson, Ark. Kemi, 23 (1964) 35.
16 Y. Shibasaki, H. Nakahara and K. Fukuda, J. Polym. Sci.: Polym. Chem. Ed., 17 (1979) 2387.
17 Y. Shibasaki and K. Fukuda, J. Polym. Sci.: Polym. Chem. Ed., 17 (1979) 2947.
18 Y. Shibasaki, J. Polym. Sci.: Polym. Chem. Ed., 18 (1980) 1693.